Macromolecules
ARTICLE

Macromolecules **2009**, *42*, 6015–6022 **6015**
DOI: 10.1021/ma9005186

Synthesis and Spectroscopic Studies of Macrocyclic Polystyrene Containing Two Fluorene Units and Single 9,10-Anthracenylidene Group

Rong Chen, Jun Ling, and Thieo E. Hogen-Esch*

Loker Hydrocarbon Research Institute and Department of Chemistry, University of Southern California, Los Angeles, California 90089-1661

Received March 10, 2009; Revised Manuscript Received July 23, 2009

ABSTRACT: The synthesis of narrow distribution model macrocyclic polystyrenes initiated with 1,4-dipotassio-bis-1,4-(9′,9′-dimethyl-2′-fluorenyl)butane (DMFB) containing 12 to 55 styrene units and coupled to a single 9,10-anthracenylidene (AN) unit (PS-DMFB-AN) is reported. The initiator is formed via electron transfer/coupling from potassium naphthalenide to give nearly pure DMFB, followed by the addition of styrene and protonation or intramolecular end-to-end coupling with 9,10-bis(chloromethyl)anthracene to give the linear and cyclic polymers, respectively. Förster transfer from the 9,9-dimethyl-2-fluorenyl (DMF) group donors to the AN groups, surprisingly, only slightly increased with lower degrees of polymerization of the PS segments. Extensive simulations indicate the presence of highly asymmetrical polymers in which the two arms of the polymer dianion significantly differ in the degree of polymerization. This appears to be partially due to chain statistics but also to slow initiation relative to polymerization.

Introduction

A great deal of research has been aimed at identifying and characterizing the active centers in photosynthesis.[1,2] Photon harvesting in polymer systems has been described and reviewed.[3−10] Early studies of the photophysics of aromatic polymers in dilute solution showed clear evidence of the occurrence of energy migration of both singlet and triplet excitons.[3,4] Singlet energy migration is believed to occur via Förster transfer, which involves dipole−dipole interactions between nearest neighboring, though not necessarily adjacent, chromophores.[11]

Synthetic polymers showing photon capture, exciton migration, and transfer to acceptor groups are intended to mimic light harvesting and have been called "antenna polymers".[5−7] A typical antenna polymer consists of a chain of monomer units containing sequences of light-absorbing chromophores (donors) and a small number of acceptor energy traps. The structure, architecture, and stereochemistry of antenna polymers has been shown to play a significant role in energy migration. For instance, polymer tacticity has been demonstrated to affect excimer formation through variation of chromophore−chromophore distances.[12]

Polyfluorenes have been studied for applications in light-emitting diodes and conducting materials, properties that relate to partial conjugation along the chain.[13−24] Poly(vinyl fluorenes) lacking this conjugation are of interest as a comparison system in the study of energy transfer in vinyl aromatic polymers.

We have recently reported the synthesis of well-defined macrocyclic 2-vinylfluorene[25−28] and similar macrocyclic vinylaromatic polymers using anionic polymerization and end-to-end coupling (Scheme 1).[29,30] These macrocycles typically show interesting increases in emission (10−50%) compared with the matching linear polymers.[26−30] In principle, methods of this type make it feasible to prepare macrocyclic polymers in which donor chromophores are separated from acceptors by a number of photochemically inert groups, allowing intramolecular "unidirectional" donor-to-acceptor energy transfer (Scheme 2).

Below, we describe the regioselective dimerization of 9,9-dimethyl-2-vinyl fluorene (DMVF) by electron transfer from potassium naphthalenide (K-Naph) to give the 1,4-dipotassio-bis-1,4-(9′,9′-dimethyl-2′-fluorenyl)butane (DMFB) as the main initiator. The initiation of styrene with the DMFB dianion and subsequent intramolecular coupling to 9,10-bis(chloromethyl)-anthracene (BCMA) gives a macrocyclic PS in which the 9,9-dimethyl-2-fluorenyl (DMF) donor (D) groups are separated from a 9,10-anthracenylidene acceptor (A) moiety by two PS "arms" containing 10−55 styrene (S) units. We also report on the intramolecular energy transfer from the fluorene (D) units to the emitting 9,10-anthracenylidene acceptor (A) group as a function of the number of styrene (S) units. These results indicate that the DPs of the two PS arms generally differ because of both Poisson distribution statistics and differences in the rates of initiation (k_i) and polymerization (k_p) (Scheme 2).

Experimental Section

Materials. We prepared potassium naphthalide (K-Naph), the initiator, by stirring naphthalene in THF over a potassium mirror for 15−20 min at 0 °C, and it was used immediately. The 9,10-bis(chloromethyl)anthracene (BCMA, TCI, 99%) coupling agent was recrystallized from $CHCl_3$ and dried under high vacuum. Styrene (Aldrich, 99%) was stirred over freshly crushed CaH_2 overnight and then vacuum distilled onto dried Bu_2Mg (1.0 M in heptane, Aldrich), from which it was distilled into ampules and diluted with solvent (hexane or THF). DMVF was synthesized and purified as reported.[29]

Polymerization and Cyclization Reactions. Polymerization and cyclization reactions were carried out as reported.[27,30,31] We prepared 1,4-dipotassio-bis-1,4-(9′,9′-dimethyl-2′-fluorenyl)butane (DMFB dianion) by slowly adding a precooled DMVF/THF solution (0.22 g, 1.12 mmol in 3 mL of THF) to about 20 mL of K-Naph/THF (0.8 mmol) solution stirred at −78 °C. After 10 min, about 90% of the living precursor dianion was poured in a flask cooled to −78 °C, to which a THF

*Corresponding author. E-mail: hogenesc@usc.edu. Fax: (213) 740-5966.

Published on Web 08/03/2009

Scheme 1. Formation of 1,4-Bis(9,9[1]-dimethyl-2-fluorenyl)butane (1,4-DMFB) Dianion, 2, the Anionic Polymerization of Styrene Giving Precursor, 4, the BCMA-Mediated Formation of Macrocycles, 5, and the Matching Linear Polymer, 6

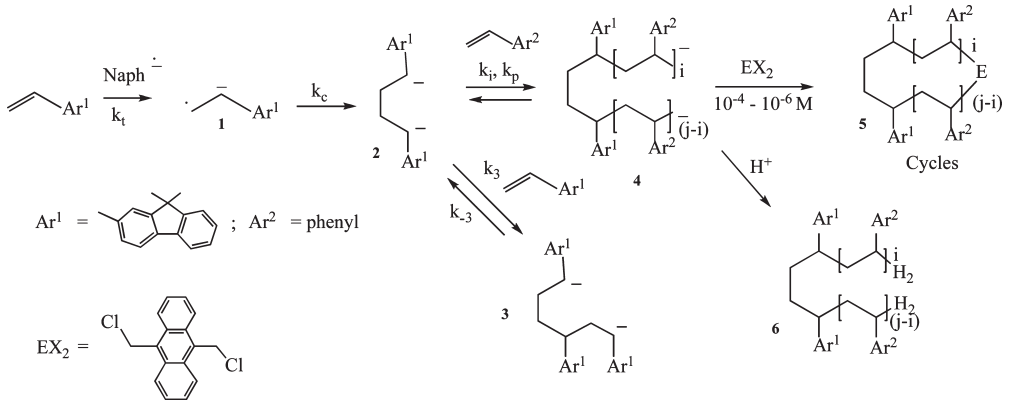

Scheme 2. "Positional" Isomers of PS Macrocycles (DP = *j*) Containing Fluorene (D) and Anthracene (A) Units with Arm Lengths of *i* and *j-i* (*i* < *j*) (See Text)

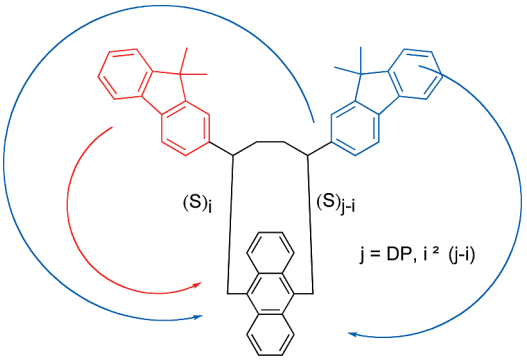

solution of styrene (1.1 g in 2 mL) was added. Then, about 80% of the resulting PS dianion solution was transferred to a precooled addition funnel kept at −78 °C at all times. Very dilute 9,10-bis(chloromethyl)anthracene (BCMA) in THF (~1.5×10^{-3} M) and the living PS dianion solution were added simultaneously dropwise to 200 mL of vigorously stirred THF at −78 °C at a rate that allowed the persistence of a very weak red color of the PS dianion and continued until the reddish color faded. The remaining 20% of the PS dianion also kept at −78 °C was then terminated with degassed methanol. The polymers were worked up and fractionated in the same way as that reported for the PDMVF homopolymer macrocycles.[32]

Characterization. Size exclusion chromatography (SEC) was carried out at 25 °C with THF as the mobile phase at a flow rate of 1 mL/min using a Waters 510 HPLC pump, a Perkin-Elmer LC-30 refractive index detector, and two Polymer Laboratories PLgel 5 μm MIXED-C columns (linear range of MW: 200−2 000 000) calibrated with polystyrene standards (Polysciences). All crude polymers were first analyzed by SEC prior to fractionation to give the correct ratios of apparent MWs of linear and cyclic polymers (Figure 1). Proton NMR was carried out on a Bruker AC 250 apparatus at 250 MHz in $CDCl_3$ and showed the expected ratios of the aromatic and aliphatic protons.

UV−vis and steady-state fluorescence emission (excited at 307 nm) measurements were typically done at a concentration of 100 mg/L in distilled cyclohexane using a Varian Cary 50 spectrometer and a PTI Quanta Master TM model C-60SE spectrofluorimeter with a 1527 PMT detector using a 3 nm slit width, respectively.

Results and Discussion

Formation of DMFB Dianion (2). The dimerization of the DMVF radical anion, **1**, formed by electron transfer to DMVF from potassium naphthalenide and subsequent coupling of the DMVF radical anion, **1**, occurred readily and nearly quantitatively to give dianion **2** (Scheme 1). This finding is significant because other vinyl aromatic monomers have not shown this curious selectivity, including α-methylstyrene. Of course, the dimerization of 1,1-diphenylentylene and 3-methyl-2-phenylbutene (MPB or α-isopropylstyrene)[32] is well known and understood because the polymerization and even trimerization of DPE and MPB are thermodynamically unfavorable as a result of significant steric hindrance in the polymer.

A similar electron-transfer-mediated regioselective synthesis of a similar butane dianion has been reported for 4-(*N*,*N*-dimethylamino)styrene (DMAS).[33] In that case, this was attributed to the excess of potassium metal that rapidly scavenges any free monomer including any monomer formed by a retroaddition of the trimer dianion. This is plausible because the polymerization of the DMAS monomer is insufficiently rapid (at least 1000 times slower than styrene) to lead to significant polymerization, which is presumably due to the electron-rich monomer.

Protonation and SEC analysis of the DMVF oligomers showed a bimodal distribution (Figure 1) with apparent SEC molecular weights (MWs) of 550 and 920 corresponding to the 1,4-bis(9′,9′-dimethyl-2′-fluorenyl) butane (1,4-DMFB) dimer along with about 0−30% of trimer (MW = 663.0 Da) formed by the addition of one DMVF to the dianion (k_3) (Scheme 1). Mass spectrometry confirmed that the DMVF oligomers mainly consisted of the DMVF dimer (MW = 442.6 Da). In one case, the 1,4-DMFB dimer dianion was exclusively formed, indicating that regioselective formation of this dianion is possible (Table 1). Other studies have shown that this is related to having a large excess of metal surface or other electron source ($Naph^{\bullet -}$) during electron transfer to the vinyl monomer and a relatively slow ($k_3 \ll k_t$) and perhaps a reversible addition of monomer compared with electron transfer and coupling (Scheme 1).[33] In the present case, the reason for the relatively slow DMVF addition, given the large size of the monomer including the two 9,9-methyl groups, should be predominantly steric rather than electronic.

In contrast with the corresponding anionic initiation/polymerization of styrene and even of α-methylstyrene and like that of DMAS, it appears to be possible to separate the initiation and polymerization processes to a significant degree. It is especially interesting that this occurred at −78 °C, well below the plausible ceiling temperature of the DMVF benzyl type monomer. Apparently, the polymerization of DMVF is slow enough to allow selective radical anion dimerization.

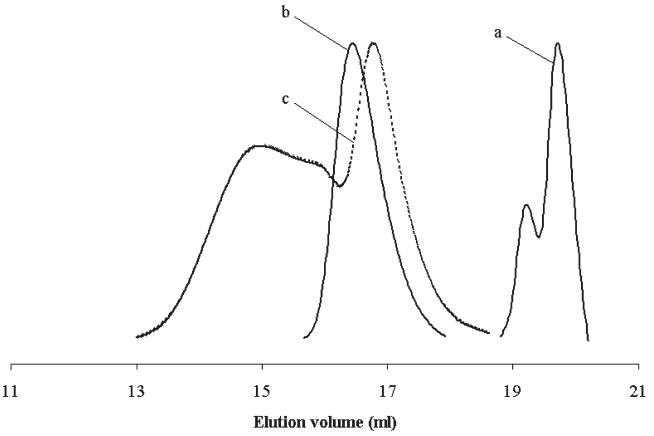

Figure 1. SEC chromatograms of (a) DMVF oligomer, (b) linear PS-DMFB-PS precursor, and (c) cyclic PS-DMFB-PS-AN (Table 1, no. II).

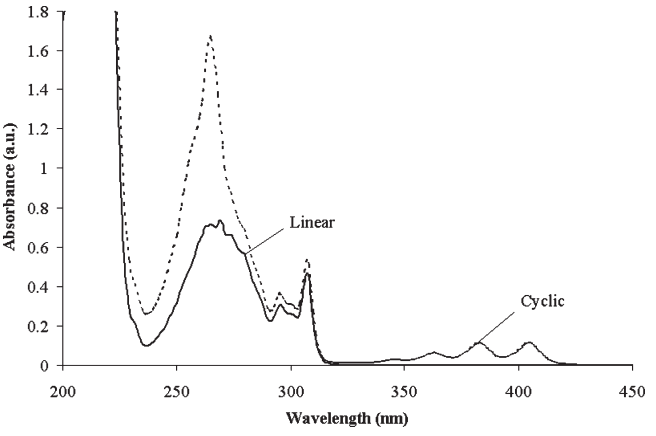

Figure 2. UV absorption spectra of linear PS-DMFB-PS (solid line) and cyclic (dotted line) PS-DMFB-PS-AN with DP_n = 29. Concentration: 100 mg/L in cyclohexane (Table 1, no. II).

Table 1. Cyclization of PDMVF-*b*-PS Coupled to BCMA at −78 °C in THF[a,b]

no.	DP_n	linear precursor			fractionated cycle			$<G>^f$
		Mp	PDI	no DMF[c]	Mp[d]	PDI	% DMA[e]	
I	12	1400	1.23	2.0	1130(1190)	1.36	78	0.85
II	29	3900	1.27	2.8	2900(3000)	1.38	74	0.77
III	55	7200	1.13	2.4	5100(5200)	1.28	76	0.72
IV[g]	44	114 200	1.10		8930(8840)	1.12	90	0.77

[a] Anion concentrations of $\sim 10^{-4}$ to 10^{-6} M. [b] MWs by SEC using PS standards. [c] Average number of DMVF units/polymer determined by NMR and SEC. [d] Values in parentheses are apparent Mp's of unfractionated cyclic PDMVF. [e] Mole % of DMA determined by UV absorptivity at 405 nm and DP_n. [f] $<G> = Mp_{(crude\ cyclic)}/Mp_{(linear)}$. [g] Linear and cyclic PDMVF homopolymers.

Polymerizations and Cyclizations. SEC analysis carried out first on the unfractionated linear and crude macrocyclic polymers indicated that the addition of styrene to the DMVF dianion, **2**, in THF at −78 °C gave relatively narrow distribution PS with apparent DP_n values ranging from 12 to 55 (Table 1). The predominant formation of the 1,4-DMFB dianion was also confirmed by ^{1}H NMR integration of the linear PS polymer that gave between 2.0 and 2.8 9,9-dimethyl-2-fluorenyl (DMF) units per chain (Table 1). Although we did not study the kinetics of formation, the 1,4-DMFB dianion, the initiation of styrene is expected to be slower than that of the anionic styrene homopolymerization because of the relatively stable 2-fluorenyl anion compared with that of the benzyl PS anion. (See below.)

Cyclizations were carried out by end-to-end coupling of the living PS dianion with BCMA at −78 °C under high dilution conditions (Figure 1, Table 1).[25] The macrocycles were fractionated by incremental additions of several small portions of methanol into its THF solution to remove higher MW products formed by inter- rather than intramolecular coupling.[25] This process was monitored by SEC after each partial precipitation and continued until the peak MWs of the purified and crude macrocyclic polymer were identical. In that stage, the purified cyclic polymers were obtained by solvent evaporation and analyzed by SEC, ^{1}H NMR, and UV/visible spectroscopy. This methodology has been shown to lead to numerous other vinylaromatic macrocycles without contamination by linear polymers.[25,30,34] Therefore, the MW distributions of the matching linear and cyclic block copolymers, obtained by SEC, were both monomodal and almost exactly the same in shape, except for the uniform shift of the entire distribution toward lower apparent MW.[25] As indicated in Figure 1, there was no evidence of the presence of low MW impurities in the linear and in the unfractionated cyclic polymers. As illustrated in the Figure, the upper parts of the MW distributions of the linear and the unfractionated polymers are essentially identical. As we have shown for the cyclic PDMVF and numerous other vinylaromatic cyclic polymers, the above synthetic and purification methods never indicated the presence of low MW impurities of any kind. Furthermore, the ratios of apparent peak MWs of the unfractionated cyclic polymers to those of the matching linear polymers, given as the $<G>$ values, increased from 0.72 (Table 1, no. I) to 0.85 (Table 1, no. III) as the molecular weights decreased. This pattern, more than any other, indicates clear evidence of the absence of linear polymers.[25] Similar trends were found for homopolymer in the same DP_n range.[25] This effect is consistent with torsional and bond angle restrictions in the smaller rings and appears to be a good indicator of the absence of appreciable fractions of linear polymer impurities.

The anthracene (A) incorporation, determined by UV absorption at 405 nm using the extinction coefficient of 9,10-dimethylanthracene (ε = 10 000)[35] varied from 74 to 78%. The apparent lower-than-calculated incorporation of the 9,10-anthracenylidene unit could be due to potassium−halogen exchange, followed by end-to-end coupling giving a cyclic polymer lacking the anthracene unit. This may be due to side reactions between BCMA and living PS dianion that can lead to slightly lower A content but without the formation of linear polymers. Alternatively, the 9,10-anthracenylidene extinction coefficients may be lower because of steric factors. (See below.) Therefore, the PDMVF-*b*-PS macrocycles have a well-defined structure with typically two 9,9-dimethyl-2-fluorenyl (DMF) chromophores on one side and one 9,10-anthracenylidene unit on the other (Scheme 1).

As illustrated in Figure 2, the UV spectra of the matching linear and cyclic PDMVF-*b*-PS with an apparent DP_n of 29 (Table 1, no. II) appeared to be very similar, showing the characteristic 9,9-dimethyl-2-fluorenyl bands at 307 and 300 nm. The macrocycle also showed absorption bands at 405, 383, and 363 nm corresponding to the 9,10-anthracenylidene linkage. Interestingly, compared with 9,10-dimethylanthracene, these bands for all macrocycles are red-shifted about 5 nm, indicating interactions between the pendent phenyl groups and the 9,10-anthracenylidene chromophore that could be consistent with hypochromic behavior.

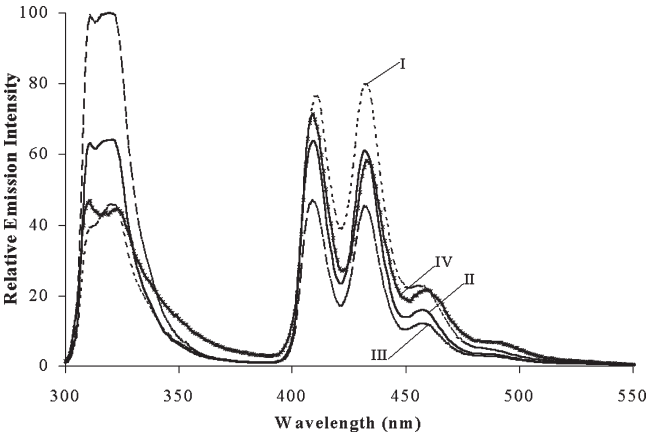

Figure 3. Fluorescence spectra of PDMVF-*b*-PS-AN macrocycles at constant concentration: of 7 mg/L (3.18×10^{-5} M in DMVF units, Table 1). (I) DP_n = 12, (dotted line), (II) DP_n = 29, (solid line), (III) DP_n = 55 (dashed line), and (IV) macrocyclic DMVF(xxx) homopolymer coupled to BCMA, DP_n = 44. Data normalized by optical density at 307 nm.

Surprisingly, in contrast with the hypochromic effect observed for the macrocyclic PDMVF homopolymer,[27] at constant overall mass, the DMF incorporated into the macrocycle showed ~17% higher absorptivity at 307 nm than the matching linear polymer and was as high as 36% for the lowest MW cycle. The reason for this apparent hyperchromicity is still not clear at present but may be related to the changed relative DMF orientations in the strained and largely flat rings. (See also below.)[36]

Emission Studies. The absorption of the DMF chromophores at 307 nm and the absence of 9,10-anthracenylidene absorption at this wavelength allow selective excitation of the DMF (D) units and energy transfer to the 9,10-anthracenylidene acceptor (A) group by observation of its emission. As shown in Figure 3, excitation at 307 nm resulted in strong 9,10-anthracenylidene emission at 409 and 432 nm and weaker bands at about 460 and 485 nm indicating effective intramolecular Förster transfer from the excited DMF donors. Reabsorption by the 9,10-anthracenylidene (AN) or DMF units was ruled out because of the low concentrations (~10^{-5} M) of donor and acceptor groups and the very low AN absorptivity between 310 and 340 nm.[24] The low concentrations of the cycles also rule out intermolecular energy transfer.

At constant DMF molar content, the emission intensity of the 9,10-anthracenylidene increased with decreasing DP of the PS ring, which is consistent with Förster transfer[11]

$$D^* + A \rightarrow D + A^* \quad (1)$$

$$k_{DA}(R) = k_D{}^0(R_0{}^{DA}/R)^6 \quad (2)$$

where R is the distance between fluorene donor (D) and anthracene acceptor (A), $k_{DA}(R)$ is the energy transfer rate, $k_D{}^0$ is the unimolecular decay rate of the donor molecule, and $R_0{}^{DA}$ is the Förster radius, the distance at which energy transfer occurs with 50% probability.

As expected, the DMF emission intensity decreased and that of the AN increased with decreasing degrees of polymerization (DP). However, the DP effects were surprisingly small (decreases of about 2.3 for DMF emission and increases of 1.7 for AN emission) given the $1/R^6$ dependence of Förster transfer.

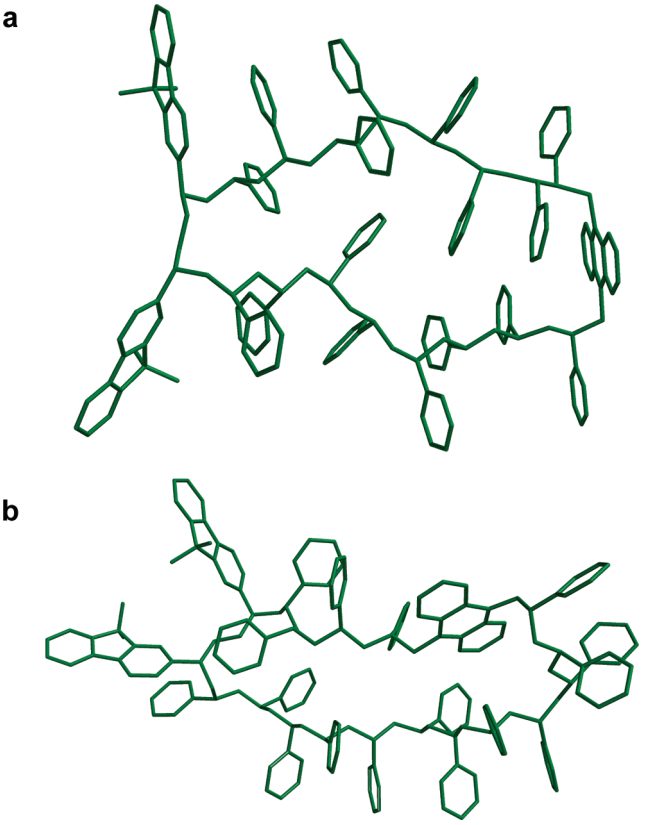

Figure 4. MM3-optimized conformation of (a) a symmetrical 8/8 heterotactic 16mer and (b) a 4/12 heterotactic 16mer.

Therefore, the donor to acceptor (D−A) distances of the above macrocycles were evaluated using MMFF and MM3 force field methods. In each case, the lowest energy cycles obtained using different building methods and starting geometries were chosen for subsequent simulations/evaluations. A truly atactic stereochemistry is not practical for force field calculations of low MW cycles of varying DPs because this leads to arbitrary differences in stereochemistry, especially for the low MW cycles. Therefore, we use a heterotactic stereochemistry to simulate the largely atactic stereochemistries obtained for PS synthesized by anionic or radical polymerizations.[37] The heterotactic $(mr)_n$ sequences for each of the two PS "arms" are arbitrarily assigned as a meso (m) dyad between the asymmetric carbon bearing the DMF unit and that of the first styrene (S) unit. The next dyad has a racemic (r) stereochemistry with the following dyad being "m" and so on, as illustrated in Figure 4 for a 16-mer having a symmetrical (8/8) and asymmetrical (4/12) placement of the 9,10-anthracenylidene acceptor (A).

Simulations were first carried out for heterotactic and symmetrical cycles (equal arm lengths) with DPs below 30. For several arbitrarily chosen atactic cycles with the same stereochemistry, the D−A distances are not very different from the heterotactic distances (within ~3%).The D−A distances were not found to be highly dependent on the tacticity (within about 5% for isotactic syndiotactic and heterotactic symmetrical 8-mers). The MMFF and MM3 simulations gave essentially identical largely "planar-rectangular" conformations. The donor-to-acceptor distances for symmetrical cycles scale linearly with DP, as shown in Figure 5. From these data and eq 2, increasing the PS number average DP (DP_n) of the cycles from 12 to 29 (Table 1) should decrease the rate of energy transfer (ETR) by a factor of $(12.7/21.1)^6$ or 4.7×10^{-2}, a value that is far lower than that observed.

There are two main causes for these low values that account for this discrepancy being related to the relative positions of both the D and the A units and are discussed in detail below. The first is statistical and based on assumed identical rates of styrene initiation (k_i) and propagation ($k_i = k_p$) (Scheme 1). This gives a Poisson distribution for a polymer with a given DP_n of both the actual DP ($= j$) distributions and that of the DPs of the two arms having DP values of i and j-i (Scheme 2). Obviously, both directly affect D−A distances. The second factor that should affect the arm DP distributions, in particular, are the probable lower rates of initiation compared with propagation ($k_i < k_p$) and possibly differences between the rates of the first and second initiations of the dianion. (See below.)

For ideal living polymerizations involving a single initiator, the DPs may be expected to follow the Poisson distribution (eq 3)[38]

$$P_j = \frac{x^{j-1}e^{-x}}{(j-1)!} \tag{3}$$

$$P_j = \frac{x^j e^{-x}}{j!} \tag{4}$$

where P_j is the mole (or number) fraction for a j-mer and x ($= DP_n$) denotes the average number of styrene (S) units that have reacted per initiator molecule. However, for the case of a dianion-initiated polymerization, the MW distributions are slightly different. In this case, the probability of zero monomer addition (DP = 0) at one of the initiator sites is finite and should be considered (eq 4). This equation also gives the distribution of symmetrical cycles where the DPs of the two PS "arms" are equal.

For the case of $DP_n = 12$ cycles, the Poisson probability maxima for the lengths of the two "arms" are seen at DPs of 5 and 6 (Figure 6).

$$P_j = \sum_{i=0}^{j} \frac{x^i e^{-x}}{i!} \cdot \frac{x^{j-i} e^{-x}}{(j-i)!} = \sum_{i=0}^{j} \frac{x^j e^{-2x}}{i!(j-i)!}$$

$$= x^j \cdot e^{-2x} \cdot \sum_{i=0}^{j} \frac{1}{i!(j-i)!} \tag{5}$$

However this is not a realistic model because the DPs of the two arms generally differ for statistical reasons (asymmetric macrocycles). Consideration of this issue leads to eq 5, where x ($= DP_n/2$) denotes the number of S units/anion and where the number of S units in each of the two arms is equal to i and j-i units, respectively.

This is illustrated in Figure 7, which gives the probability distribution of the DPs of the shorter arms for macrocycles having DPs of 12 and 18 styrene units. Therefore, for the 12-mer, there is one symmetrical (6/6) cycle, that is, $i = (j\text{-}i) = 6$, along with the six "asymmetric" 5/7, 4/8, 3/9, 2/10, 1/11, and 0/12 cycles, where the first number corresponds to the shorter arm. Likewise, for the $DP_n = 18$ case, the probability for the asymmetrical cycles exceeds that for the symmetrical ones by about a factor of four (Figure 7).

Because the asymmetrical cycles will also have shorter D−A distances than the symmetrical ones for both fluorene donors, they should contribute even more to the D−A transfer rates. The molecular-mechanics-based D−A distances between the A unit and the closer and more distant D units for the cycles with DPs of 12, 14, 16, and 18 scale in

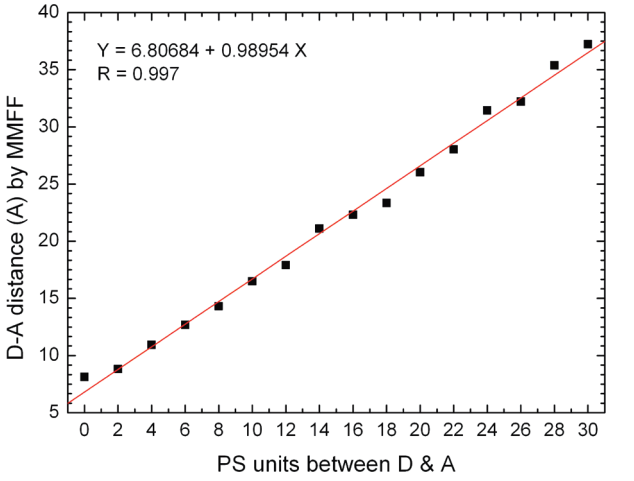

Figure 5. Dependence of DA distances on number of S units for the case of symmetrical cycles. Data obtained by MMFF force field calculations.

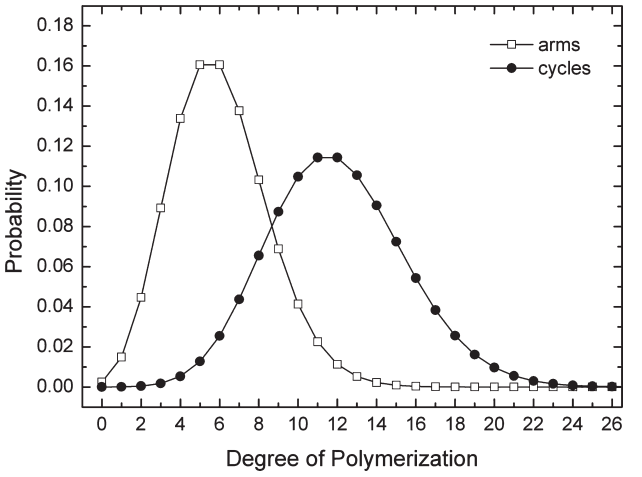

Figure 6. Poisson distributions for a $[M]_0/[\text{dianion initiator}]_0$ ratio of 12. The probability distributions of S units in arms (□) and in macrocycles (●) were obtained from eqs 3 and 4, respectively.

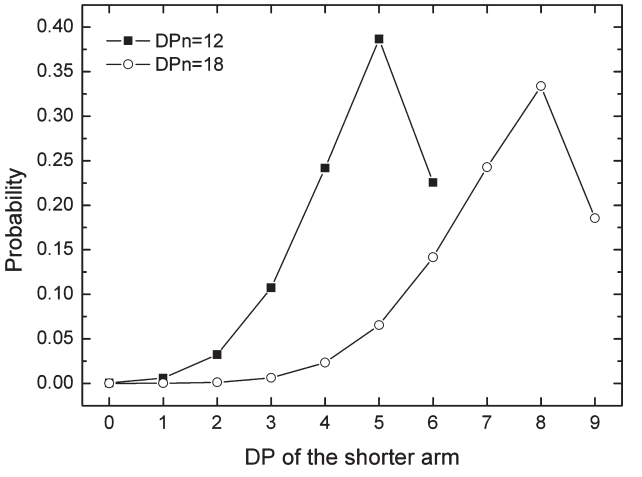

Figure 7. Probabilities of positional cyclic isomers for a DP = 12 cycle (■) and for a DP = 18 cycle (○). The horizontal axis denotes the number of S units in the shorter arm. The lines are used for visual guidance.

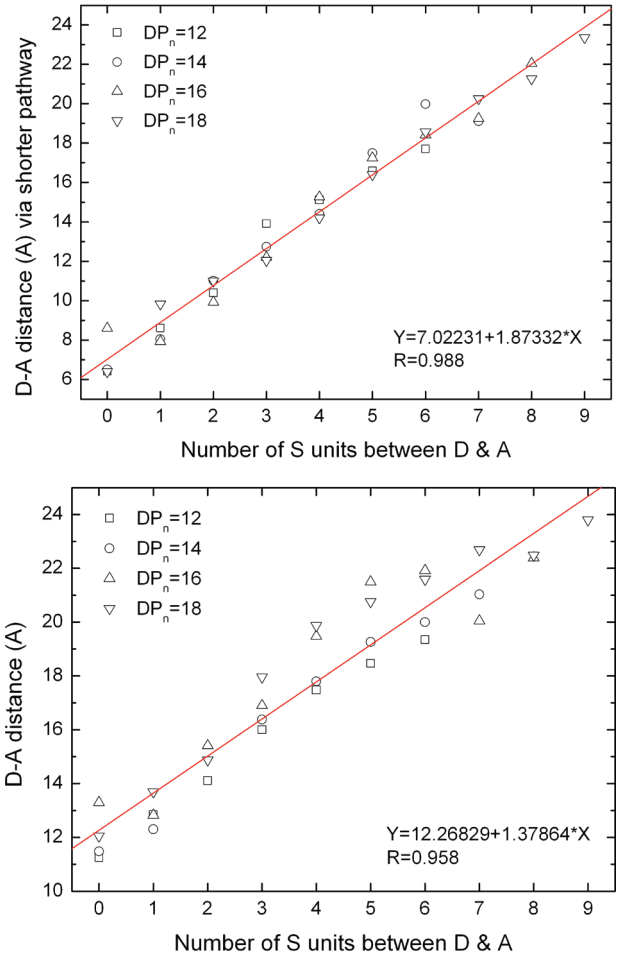

Figure 8. (a) Linear fit of D−A distances of the closer D unit (shorter arm) for the heterotactic 12-, 14-, 16-, and 18-mers (MMFF simulations). (b) Linear fit of the distance between the "distant" donor as a function of the shorter arm DP (MMFF simulations).

roughly linear fashion, as illustrated in Figure 8a,b respectively. The resulting expected energy transfer rates (ETRs) are calculated using the sum of the Förster rates for the shorter ($R_{i,\mathrm{short}}$) and longer ($R_{i,\mathrm{long}}$) D−A distances, respectively (eq 6). For the case of the $\mathrm{DP}_n = 12$ distribution of cycles, the resulting ETRs are illustrated in Figure 9.

$$\mathrm{ETR}_j = \sum_{i=0}^{j/2} \mathrm{ETR}_{i/(j-i)} = \sum_{i=0}^{j/2} P_{i/(j-i)} \left(\frac{1}{R^6_{i,\,\mathrm{short}}} + \frac{1}{R^6_{i,\,\mathrm{long}}} \right) \qquad (6)$$

This and similar "bubble" plots for the $\mathrm{DP}_n = 18$, 28, and 54 cycles (Figures S-1 to S-3, respectively, in the Supporting Information) illustrate the simulated contributions to the Förster transfer rates, where the x and y axes indicate the total number of S units in the cycles and the number of S units in the shorter arms. As seen in Figure 9, the ETR is mostly due to 1-, 2-, 3-, and 4-mer arms with a not insignificant contribution of the $j = 0$ arm. This clearly illustrates that the smaller and especially the highly asymmetrical cycles tend to dominate ETR. This is not so evident for the 18-, 28-, and 54-mers that give a far smaller energy transfer (sum ETR, factors of $10-10^4$) (Figures S-1 to S-3 in the Supporting Information). This is

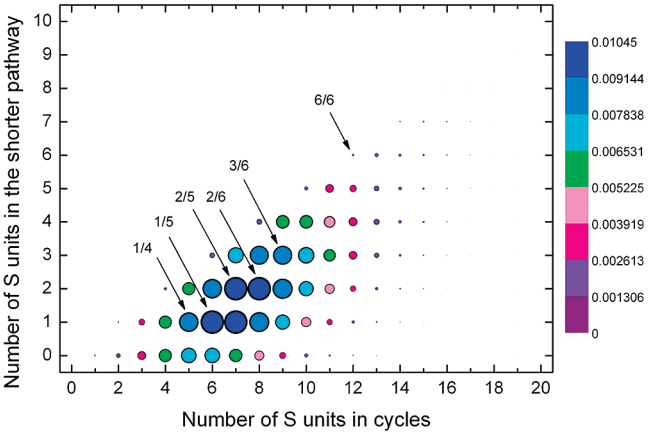

Figure 9. Bubble plot of $\mathrm{ETR}_{i/(j-i)}$ as function of the total number of S units in the $\mathrm{DP}_n = 12$ cycle population and number of S units in the shorter arms.

Scheme 3. Initiation of Styrene by Dianions 2−4

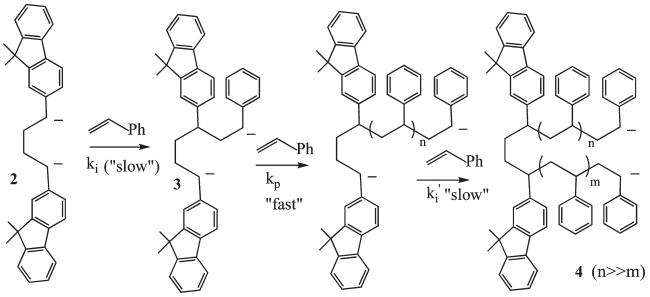

inconsistent with the experimental results that show roughly comparable rates of energy transfer (factors of about two) for the 9,10-anthracenylidene and 9′,9′-dimethyl-2′-fluorenyl emissions (Figure 3).

The above indicates that other factors could be involved in the formation of highly asymmetric cycles. First, there should be differences in the rates of styrene initiation and polymerization. The initiation of styrene with the DMF anion (k_i) should be slower than that of the PS benzyl anion (k_{ST}) because of the increased anion stabilization caused by the presence of a second coplanar phenyl ring (Scheme 3). Also, initiation by the two DMF anions may be expected to have different initiation rates because of the electrostatic repulsion in the initiating dianion. (See below.) In the following, we discuss these factors, especially the first, in some detail.

To our knowledge, the anion stability of the 2-alkylfluorenyl anion is not known. A conservative estimate of the pK_a difference of 4-ethylbiphenyl relative to toluene has been shown to be 2.6 using the Cs/cyclohexylamide system.[39] Therefore, the basicity of the PS anion should be appreciably larger than that of the 4-ethylbiphenyl anion. Furthermore, the 2-fluorenyl anion is expected to be more stable than the 4-ethylbiphenyl anion because of the enhanced conjugation provided by the second ring that is coplanar to the first. This is likely to give even lower rates of styrene addition relative to PS anion ($k_i \ll k_p$) (Scheme 3). Although no kinetic data are available for the current system, the addition of styrene to the analogous 1-alkylnaphthalene anion is roughly 30 times slower compared with that of the PS anion in THF in the presence of Na ion.[40]

Finally, the initiation rates of the DMF anions in the dianion initiator have been assumed to be equal ($k_i = k_i'$, Scheme 3). This may not be the case because the electrostatic

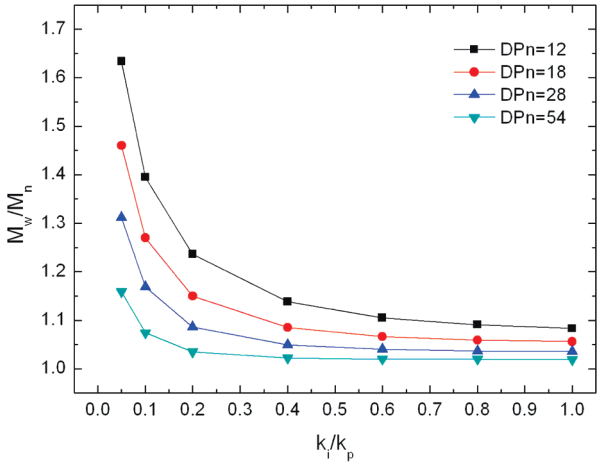

Figure 10. Dependence of M_w/M_n on k_i/k_p (based on MC simulations).

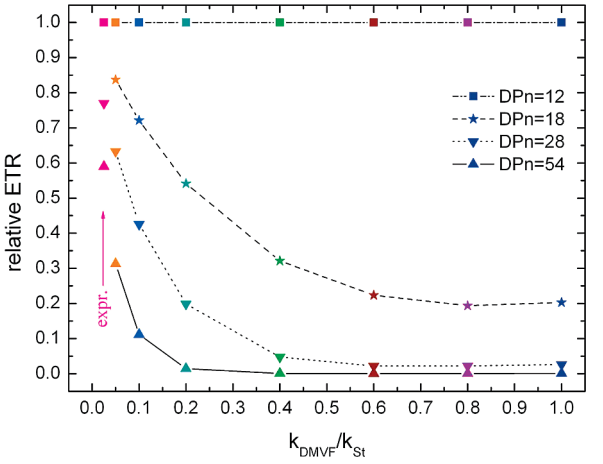

Figure 11. Relative values of "sumETR" versus the k_i/k_p value plot by setting sumETR value of DP_n = 12 to 1.00. The red points correspond to the experimental data.

repulsion of the two anions would tend to cause differences in reactivity as the initiation of styrene moves the negative charge of the newly formed PS anion, **3**, further away from the remaining 2-fluorenyl anion. An indication that this may be the case is consistent with conductance studies of analogous bola-form Cs electrolytes in THF of the type Cs^+, $Flu^-(CH_2)_nFlu^-,Cs^+$ where Flu^- represents the 9-fluorenyl anion and the number, n, of methylene groups linking the two 9-fluorenyl positions varies from 2 to 6. The first dissociation step forming the Cs^+ and the triple anion ($M^+,Flu^-(CH_2)_nFlu^-,M^+ \leftrightarrows M^+,Flu^-(CH_2)_nFlu^- + M^+$) is significantly greater than the second dissociation step (factors of 2−12).[41,42] This suggests that the reactivity of the two anions should also differ. If our initiation rates are mediated through free anions, then the reactivity of the triple anion with one cation shielding two anions should be greater than that of the remaining ion pair, and this should cause even greater differences in the relative sizes of the two PS arms (ring "asymmetry").[40]

Monte Carlo (MC) methods (Figure S-4 in the Supporting Information) (consistent with Poisson statistics for the case that $k_i/k_p = 1$) were used to obtain changes in MW distributions as a function of k_i/k_p, assuming that $k_i = k_i'$ (Figure 10). The corresponding changes in ETR ("sumETR") are shown in Figure 11, keeping the experimental sum ETR (anthracene emission) values at 1.0 for the DP =12 cycles. Given the moderately narrow experimental MW distributions of the linear precursors, the MW distribution data are consistent with a value of k_i/k_p on the order of 0.1 to 0.2. However, the actual differences in arm lengths may be larger because our SEC data do not give relative PS arm lengths. This is consistent with highly asymmetrical cycles and gives a reasonable account for the relatively small differences in energy transfer among the macrocycles for small values of k_i/k_p ($0.05 < k_i/k_p < 0.20$). Support for this interpretation is also suggested by the anthracene emission of the cyclic PDMVF homopolymer that is actually lower than that for sample I, indicating that the energy transfer may be primarily due to 2-fluorene units being adjacent to the anthracenylidene unit.

In conclusion, we have shown the regioselective formation of tail-to-tail DMF dianion and its initiation of styrene and intramolecular coupling with 9,10-bis (chloromethyl)-anthracene to give the corresponding PS macrocycles having two 9,9-dimethyl-2-fluorenyl donors and one 9,10-anthracenylidene acceptor group. Surprisingly, small differences in Förster transfer rates with ring size indicate that this primarily may be due to highly asymmetric cycles in which the units are in very close proximity to both of the 9,9-dimethyl-2-fluorenyl donors. This appears to be due to both the chain statistics that favor asymmetric cycles and the very low rates of initiation compared with those of propagation.

Acknowledgment. This work was partially supported by NSF-STC 594068, NSF-DMR 9810283, and the Loker Hydrocarbon Research Institute. We thank Stephen Bradforth for the use of the UV spectrometer and Mark Thompson for the use of his spectrofluorimeter and mass spectrometer.

Supporting Information Available: Dependence of D−A distances on the DPs of heterotactic polystyrene macrocycles containing a 9,10- anthracenylide unit separated from the two DMF units by arms of equal length, D−A distance from two different donors to the acceptor in asymmetric 12-, 14-, 16-, and 18-mers, bubble plots of $ETR_{i/(j-i)}$, and flow chart of Monte Carlo simulation. This material is available free of charge via the Internet at http://pubs.acs.org.

References and Notes

(1) (a) Van Grondelle, R. *Adv. Photosynth. Respir.* **2009**, 231–252. (b) Zouni, A.; Witt, H. T.; Kern, J.; Fromme, P.; Krauss, N.; Saenger, W.; Orth, P. *Nature* **2001**, *409*, 739–743. (c) Ferreira, K. N.; Iverson, T. M.; Maghlaoui, K.; Barber, J.; Iwata, S. *Science* **2004**, *303*, 1831–1838.
(2) Van Grondelle, R.; Dekker, J. P.; Gilbro, T.; Sundstrom, V. *Biochim. Biophys. Acta* **1994**, *1187*, 1–65.
(3) Fox, R. B.; Cozzens, R. F. *Macromolecules* **1969**, *2*, 181–184.
(4) Schneider, F.; Springer, J. *Makromol. Chem.* **1971**, *146*, 181–193.
(5) Webber, S. E. *Macromol. Symp.* **1999**, *143*, 359–370.
(6) (a) Guillet, J. E. Chapter 9. In *Polymer Photophysics and Photochemistry*; Cambridge University Press: Cambridge, U.K., 1985. (b) Guillet, J. *Trends Polym. Sci.* **1996**, *4*, 41–46.
(7) Phillips, D.; Rumbles, G. *Polym. Photochem.* **1984**, *5*, 153–170.
(8) Semerak, S. N; Frank, C. W. *Adv. Polym. Sci.* **1984**, *54*, 31–85.
(9) Ghiggino, K. P. *Makromol. Chem., Macromol. Symp.* **1992**, *53*, 355–365.
(10) Carey, M. J.; Phillips, D. *Chem. Phys.* **1994**, *185*, 75–89.
(11) Förster, Th. *Ann. Phys.* **1948**, *437*, 55–75.
(12) (a) David, C.; Putman-de Lavarielle, N.; Genskens, G. *Eur. Polym. J.* **1974**, *10*, 617–621. (b) Ishii, T.; Handa, T.; Matsunaga, S. *J. Polym. Sci., Polym. Phys. Ed.* **1979**, *17*, 811-823. (c) Boudevsha, H.; Brutchkov, C. *Makromol. Chem.* **1979**, *180*, 1113–1117.
(13) Janietz, S.; Bradley, D. D. C.; Grell, M.; Giebeler, C.; Inbasekaran, M.; Woo, E. P. *Appl. Phys. Lett.* **1998**, *73*, 2453–2455.
(14) Grell, M.; Bradley, D. D. C.; Ungar, G.; Hill, J.; Whitehead, K. S. *Macromolecules* **1999**, *32*, 5810–5817.
(15) Teetsov, J.; Fox, M. A. *J. Mater. Chem.* **1999**, *9*, 2117–2122.
(16) Somma, E.; Loppinet, B.; Chi, C.; Fytas, G.; Wegner, G. *Phys. Chem. Chem. Phys.* **2006**, *8*, 2773–2778.
(17) Klaerner, G.; Miller, R. D. *Macromolecules* **1998**, *31*, 2007–2009.

(18) (a) Pei, Q. B.; Yang, Y. *J. Am. Chem. Soc.* **1996**, *118*, 7416–7417. (b) Scherf, U.; List, E. J. W. *Adv. Mater.* **2002**, *14*, 477–487.
(19) Kreyenschmidt, M.; Klaerner, G.; Fuhrer, T.; Ashenhurst, J.; Karg, S.; Chen, W. D.; Lee, V. Y.; Scott, J. C.; Miller, R. D. *Macromolecules* **1998**, *31*, 1099–1103.
(20) Gross, M.; Muller, D. D.; Nothofer, H. G.; Scherf, U.; Neher, D.; Brauchle, C.; Meerholz, K. *Nature* **2000**, *405*, 661–665.
(21) Yan, J. C.; Cheng, X.; Zhou, Q. L.; Pei, J. *Macromolecules* **2007**, *40*, 832–839.
(22) Cotts, P. M.; Swager, T. M.; Zhou, Q. *Macromolecules* **1996**, *29*, 7323–7328.
(23) Grimsdale, A. C.; Mullen, K. *Adv. Polym. Sci.* **2006**, *199*, 1–82.
(24) Ranger, M.; Rondeau, D.; Leclerc, M. *Macromolecules* **1997**, *30*, 7686–7691.
(25) Hogen-Esch, T. E. *J. Polym. Sci., Part A: Polym. Chem.* **2006**, *44*, 2139–2155 and references therein.
(26) Johnson, J. M.; Chen, R.; Chen, X.-Y.; Moskun, A. C.; Zhang, X.; Hogen-Esch, T. E.; Bradforth, S. E. *J. Phys. Chem B* **2008**, *112*, 16367–16381.
(27) Chen, R.; Johnson, J.; Bradforth, S. E.; Hogen-Esch, T. E. *Macromolecules* **2003**, *36*, 9966–9970.
(28) Chen, R.; Nossarev, G. G.; Hogen-Esch, T. E. *Makromol. Chem., Macromol. Symp.* **2004**, *215*, 67–79.
(29) Chen, R.; Zhang, X.; Hogen-Esch, T. E. *Macromolecules* **2003**, *36*, 7477–7483.
(30) Alberty, K. A.; Tillman, E.; Carlotti, S.; King, K.; Bradforth, S. E.; Hogen-Esch, T. E.; Parker, D.; Feast, W. J. *Macromolecules* **2002**, *35*, 3856–3865.
(31) Alberty, K. A.; Hogen-Esch, T. E.; Carlotti, S. *Macromol. Chem. Phys.* **2005**, *206*, 1035–1042.
(32) Alberty, K.; Chen, R.; Hogen-Esch, T. E. *J. Polym Sci., Part A: Polym. Chem.* **2002**, *40*, 2108–2115.
(33) Warner, W.; Hogen-Esch, T. E. *Macromolecules* **2002**, *35*, 3787–3789.
(34) Nossarev, G. G.; Tillman, E.; Hogen-Esch, T. E. *J. Polym. Sci., Part A: Polym. Chem.* **2001**, *39*, 3121–3129.
(35) (a) Tillman, E. S.; Hogen−Esch, T. E. *Macromolecules* **2001**, *34*, 6616–6622. (b) Tillman, E. S.; Hogen-Esch, T. E. *J. Polym. Sci., Part A: Polym. Chem.* **2002**, *40*, 1081–1091.
(36) Cantor, C. R.; Schimmel, P. R. Chapter 7. In *Biophysical Chemistry Part II: Techniques for the Study of Biological Structure and Function*; W. H. Freeman: San Francisco, 1980.
(37) Bywater, S. Chapter 28. In *Comprehensive Polymer Science: Chain Polymerization I*; Eastmond, G. C., Ledwith, A., Russo, S., Sigwalt, P., Eds.; Pergamon Press: Elmsford, NY, 1989; Vol. *3*, p 433.
(38) (a) Flory, P. J. Chapter VIII. In *Principles of Polymer Chemistry*; Cornell University Press: Ithaca, NY, 1953. (b) Morton, M. Chapter 8. In *Anionic Polymerization: Principles and Practice, Part II*; Academic Press: New York, 1983.
(39) Streitwieser, A.; Guibe, F. *J. Am. Chem. Soc.* **1978**, *100*, 4532–4534.
(40) Szwarc, M. *Carbanions, Living Polymers, and Electron Transfer Processes*; Interscience Publishers: New York, 1968; p 544.
(41) Collins, G. L.; Smid, J. *J. Am. Chem. Soc.* **1973**, *95*, 1503–1508.
(42) Collins, G. l.; Hogen- Esch, T. E. *J. Solution Chem.* **1978**, *7*, 9–18.